Accepted Manuscript

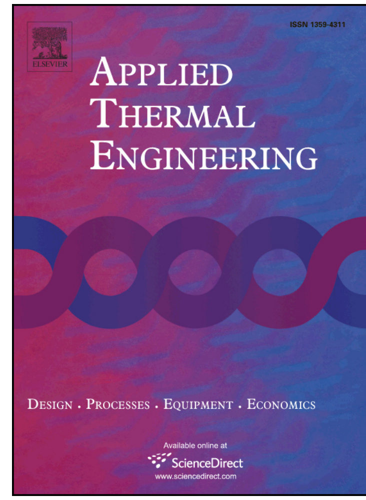

Simultaneous heat and water recovery from flue gas by membrane condensation: Experimental investigation

Shuaifei Zhao, Shuiping Yan, David K. Wang, Yibin Wei, Hong Qi, Tao Wu, Paul H.M. Feron

PII: S1359-4311(16)33276-8
DOI: http://dx.doi.org/10.1016/j.applthermaleng.2016.11.101
Reference: ATE 9512

To appear in: *Applied Thermal Engineering*

Received Date: 8 September 2016
Revised Date: 12 November 2016
Accepted Date: 13 November 2016

Please cite this article as: S. Zhao, S. Yan, D.K. Wang, Y. Wei, H. Qi, T. Wu, P.H.M. Feron, Simultaneous heat and water recovery from flue gas by membrane condensation: Experimental investigation, *Applied Thermal Engineering* (2016), doi: http://dx.doi.org/10.1016/j.applthermaleng.2016.11.101

Simultaneous heat and water recovery from flue gas by membrane condensation: Experimental investigation

In preparation for

Applied Thermal Engineering

Shuaifei Zhao [a,b,]*, Shuiping Yan [c], David K. Wang [d], Yibin Wei [a], Hong Qi [e,]**, Tao Wu [f], Paul H.M. Feron [b]

[a] *Department of Environmental Sciences, Macquarie University, Sydney, NSW 2109, Australia*

[b] *CSIRO Energy, P.O. Box 330, Newcastle, NSW 2300, Australia*

[c] *College of Engineering, Huazhong Agricultural University, Wuhan 430070, China*

[d] *The University of Queensland, FIM²Lab - Functional Interfacial Materials and Membranes Laboratory, School of Chemical Engineering, Brisbane QLD 4072, Australia*

[e] *State Key Laboratory of Materials-Oriented Chemical Engineering, Membrane Science and Technology Research Centre, Nanjing Tech University, Nanjing 210009, China*

[f] *Ocean College, Zhejiang University of Technology, Hangzhou, 310032, China*

* *Tel. +61-2-9850-9672; email: shuaifei.zhao@mq.edu.au; zhasy001@mymail.unisa.edu.au*

** *Tel. +86-25-83172279; e-mail: hqi@njtech.edu.cn*

Abstract

A tubular ceramic membrane is investigated as the condenser for simultaneous heat and water recovery from flue gas. The effects of the operational parameters, such as fluid (gas and water) flow rates, temperatures of flue gas and coolant water, and flue gas humidity on the process performance in terms of mass and heat transfer across the membrane are studied. Particularly, the overall heat transfer coefficient is also evaluated. As the gas flow rate increases, water and heat transfer efficiencies and recoveries decline due to the reduced residence time. Increasing the water flow rate or lowing the coolant temperature can effectively improve mass and heat transfer efficiencies and recoveries. Increasing the temperature of the inlet gas can enhance water and heat fluxes and recoveries, but does not improve the overall heat transfer efficiency. The rise in flue gas humidity can dramatically improve water and heat transfer rates and the overall heat transfer coefficient, but has little effect on water and heat recoveries. These results offer a general guideline in optimising the operational parameters in low-grade heat recovery with membrane heat exchangers, and it may greatly advance the development of membrane condensation technology for practical low-grade heat recovery.

Key words: Flue gas; low-grade heat; heat recovery; water recovery; membrane condenser; heat transfer.

1. Introduction

As our world is experiencing energy shortages, utilization of low-grade heat has attracted growing interest [1]. Flue gas from fossil fuel fired power plants is one of the low-grade heat sources of great interest [2-4]. Wet exhaust flue gas typically has high temperature and moisture, making it a potential source for both energy and water.

The temperature of flue gas varies significantly, depending on the measurement distance from the boiler and the types of power plants. For a coal-fired power plant, generally the flue gas temperature is below 130 °C, and the flue gas contains 10 - 16% (v/v) water vapor with considerable latent heat. There is no doubt that direct emission of exhaust flue gas into the air causes the waste of energy and water. Considerable energy would be saved if partial waste heat can be recovered from flue gas. It is estimated that 35 million tons of standard coal can be saved annually if half of the latent heat in the flue gas can be recovered [5].

On the other hand, large quantity of water is consumed in power plants, and power plants could be self-sufficient with water if 20% of water vapor in flue gas can be captured [6]. Therefore, recovering low-grade heat and/or water vapor from flue gas has been a technical challenge for the science and engineering communities and industry [5, 7-10].

Several technologies, such as organic Rankine cycle (ORC) [2, 11, 12], absorption systems [13], condensation methods [3, 14], waste heat boilers and heat exchangers [9, 15, 16], have been studied for waste heat and/or water recovery from exhaust gas. However, these methods have their limitations in practical low-grade heat recovery from power plants. For example, ORC systems require extra heat to preheat the ORC working fluid. The relatively low temperature of flue gas also limits the efficiency of using conventional heat exchangers and thus requires large surface areas. High regeneration cost makes the adsorption method too expensive. Efficient alternative technologies are highly needed for recovering the low-grade heat and water vapor from flue gas.

One of the most promising technologies, membrane condensation, has emerged to recover heat and water from wet exhaust flue gas from coal-fired power plants [17-19]. Membrane condensers as novel heat exchangers can overcome the disadvantages of conventional technologies (e.g. corrosion, fouling and high energy consumption [14]) in water and heat recovery [10, 20-22]. A membrane heat exchanger may also offer higher heat recovery efficiency than conventional heat exchangers because both mass and heat transfer occurs across the membrane [23].

Two types of membrane condensers based on different mechanisms have been employed for heat and/or water recovery from flue gas. Wang et al. [8, 10] developed hydrophilic ceramic membranes as transport membrane condensers for water and heat recovery from flue gas, where water vapor transfers through the membrane via capillary condensation. The recovered heat and water can be used for boiler makeup water. More recently, this condensation technology has been used for water recovery from internal combustion engine exhaust gas [24] and heat recovery in carbon capture [25]. Macedonio et al. [20-22, 26] employed hydrophobic porous polymer membranes for water recovery from flue gas, where water vapor condenses and is then collected on the feed side and non-condensable gases permeate through the membrane.

In our previous studies, saturated gas streams at relatively low temperatures (< 85 °C) were studied with both monochannel and multichannel ceramic tubes [19, 27]. In the current work, we employ a new method to generate simulated flue gas (relatively humidity: 11-14 vol.% at 100 °C) and explores the feasibility of employing nanoporous tubular ceramic membranes for simultaneous water and heat recovery from simulated flue gas. Influences of operational parameters, such as gas flow rate, coolant water flow rate, inlet gas temperature, coolant water temperature and flue gas humidity on process performance are investigated. This study offers a guideline in optimising the operational parameters in low-grade heat recovery with membrane heat exchangers, and it may greatly advance the development of membrane condensation technology for practical heat and water recovery from power station flue gas.

2. Materials and methods

2.1. Membrane preparation

We prepared membranes using the method that can be found elsewhere [28]. Briefly, titania sol was synthesized through the colloidal sol-gel method. The prepared sol was coated on a tubular α-Al_2O_3 mesoporous support via dip-coating [29], and then calcined at 400 °C for 3 h. The support (OD: 12 mm, ID: 8 mm, length: 85 mm, average pore size: 20 nm) was obtained from Jiangsu Jiuwu Hi-tech Co. China.

The tubular ceramic membrane has its separation layer on the inner side, and its thickness is ~100 nm. Average pore size of the separation layer is ~7 nm, based on the gas bubble method [30, 31]. The ceramic membrane has an effective area of 0.0021 m^2.

2.2. Flue gas

Simulated flue gas containing air and water vapor was produced by the following system. Measured water vapor contents within the simulated flue gas (i.e. humidity ratios) were 85 - 100 g/kg, which corresponds to 11-14 vol.% in flue gas at 100 °C. Humidified air has been simulated as engine exhaust gas in a similar lab-scale investigation [24].

2.3. Experimental setup

A bench-scale setup was designed for artificial flue gas generation and heat and water recovery (Fig. 1). First, dry air was humidified and preheated with a heating water bath, and its flow rate was measured by a mass flow controller (Bronkhorst High-Tech). The humidified air flowed into a steam generator (HGA-M-01, United States) coupled with a temperature and power control system by which the flue gas temperature from the steam generator and the input power could be finely controlled. The generated artificial flue gas (i.e. air and water vapor) flowed into tube side of the membrane. The humidity of inlet flue gas was monitored by a humidity transmitter (HMT337, Vaisala, Finland) and the gas temperature was measured with a thermocouple. Cold water countercurrently flowed on the shell side of the ceramic tube. The whole system was thermally insulated.

Temperature of the coolant water increased gradually due to the transferred heat from the hot gas side. Heat transfer can be determined based on the flow rate, inlet and outlet temperatures of water. Mass transfer can be calculated according to the weight change of the liquid water with a balance. When mass transfer and heat transfer became relatively steady, data recording was commenced. The time to reach a relatively steady state varied from 20 to 50 min depending on the experimental conditions. For each experimental condition, the weight and temperature data were recorded for 50 min at a time interval of 2 min.

2.4. Flux and recovery determination

In a membrane heat changer, simultaneous mass and heat transfer occurs across the membrane. Water and heat fluxes and recoveries are important parameters for assessing the membrane process performance.

Water flux (J_w) and heat flux (q) can be respectively described by

$$J_w = \frac{\Delta W}{\Delta t\ A} \qquad (1)$$

$$q = \frac{C\,\dot{m}_l\,\Delta T + \dot{m}_T h(T)}{A} \quad (2)$$

where ΔW is the weight change (kg) of the liquid water during a time period Δt (h), A is the effective membrane area (m^2), C is the specific heat capacity of water ($kJ \cdot kg^{-1} \cdot K^{-1}$), $\dot{m}_l$ is the liquid coolant (water) flow rate ($kg \cdot h^{-1}$) and ΔT is the temperature change of the liquid water (K), $\dot{m}_T$ is the water transfer rate, ΔW/Δt ($kg \cdot h^{-1}$), and h(T) is the water specific enthalpy ($kJ \cdot kg^{-1}$) at temperature T.

Water recovery (γ) can be expressed by

$$\gamma\,(\%) = \frac{\Delta W}{W_{inlet}} \times 100 = \frac{\Delta W}{\omega \dot{m}_{air} \Delta t} \times 100 \quad (3)$$

where W_{inlet} is the inlet water content (kg) of the gas stream during the same time period as ΔW, ω is the humidity ratio ($kg \cdot kg^{-1}$), and $\dot{m}_{air}$ is the dry air flow rate ($kg \cdot h^{-1}$). The values of ω and $\dot{m}_{air}$ can be experimentally determined by the humidity transmitter and mass flow controller, respectively.

Heat recovery (η) can be determined by

$$\eta\,(\%) = \frac{U_{obtain}}{U_{inlet}} \times 100 = \frac{q\,A}{h \dot{m}_{inlet}} \times 100 \quad (4)$$

where U_{obtain} is the obtained heat transfer rate ($kJ \cdot h^{-1}$) across the membrane, U_{inlet} is the heat flow rate ($kJ \cdot h^{-1}$) of the inlet gas stream to the membrane module, h is the specific enthalpy ($kJ \cdot kg^{-1}$) of the gas stream, and $\dot{m}_{inlet}$ is the gas stream flow rate ($kg \cdot h^{-1}$). Both h and $\dot{m}_{inlet}$ can be obtained from the Humidity Calculator software from Vaisala, Finland.

2.5. Overall heat transfer coefficient calculation

Heat transfer in the membrane condenser is complex because it involves both convective and conductive heat transfer. To simplify the situation, we employ the overall heat transfer coefficient U (in $W{\cdot}m^{-2}K^{-1}$), which accounts for the membrane resistance and all other external factors (e.g. the boundary layer effect). The overall heat transfer coefficient is an effective parameter indicating the heat transfer performance of the membrane condenser. The overall heat transfer coefficient is given by

$$U = \frac{q}{A\,\Delta T} \tag{5}$$

where

$$\Delta T = \frac{(T_{h,in} - T_{c,out}) - (T_{h,out} - T_{c,in})}{\ln\left(\frac{T_{h,in} - T_{c,out}}{T_{h,out} - T_{c,in}}\right)} \tag{6}$$

ΔT is a logarithmic mean temperature difference (K), commonly used in counter-current heat exchange, and $T_{h,in}$, $T_{h,out}$, $T_{c,in}$ and $T_{c,out}$ are the temperatures (K) of the inlet hot stream, outlet hot stream, inlet cold stream and outlet cold stream, respectively. These temperatures were experimentally measured with in-line thermocouples.

3. Results and discussion

3.1. Effect of gas flow rate

Fig. 2A shows that both water and heat fluxes decrease with the increase in gas flow rate. Interestingly, it appears that this trend is against the boundary layer heat and mass transfer theory, and is totally different from previous results using water vapor saturated gas stream as the feed [19, 23, 27]. Mass and heat transfer rates should increase or be relatively stable with the rise in fluid flow rate when the boundary layer effect is significant or insignificant, respectively [32-35]. However, the trend can be explained by the data in Fig. 2B, where the humidity ratio and specific enthalpy of the flue gas decline with the increase in gas flow rate. Namely, the water vapor quantity and heat content within the flue gas decrease due to the reduced air residence time in the humidifier when increasing the air flow rate. As a result, mass and heat transfer rates decline with the increase in the gas flow rate (Fig. 2A).

Similar to the transfer rates, both water recovery and heat recovery decrease with the increase in the gas flow rate (Fig. 2C). When the gas flow rate increases from 2.7 to 6.7 L min^{-1}, water recovery decreases from 37% to 23% and heat recovery decreases from 35% to 19%. These results indicate that higher water and heat recoveries can be achieved at lower feed flow rates due to longer residence time, and higher humidity and specific enthalpy within the flue gas. Compared with the recovery performance from saturated gas streams, water and heat recoveries from unsaturated flue gas with the same type of membranes are much lower [19].

In practical heat and water recovery from flue gas, mass and heat transfer rates across the membrane condenser are more likely to increase with the increase of the flue gas flow rate since the humidity and enthalpy of the flue gas from a given power plant are relatively stable. However, the transfer rates may vary with the properties of the flue gas from different power plants. Heat and water recoveries could be improved due to the increased residence time when longer tubular membranes are used [24]. Note that we select the dry air flow rate rather than wet gas mixture (i.e. air and water vapor) flow rate as a parameter because it is impractical to experimentally measure the wet gas flow rate due to surface condensation.

Fig. 2D shows the effect of gas flow rate on the overall heat transfer coefficient. As expected, the overall heat transfer coefficient reduces with the increase in gas flow rate because of the lower specific enthalpy at higher gas flow rates. Within the experimental gas flow rate range, the overall heat transfer coefficients vary from 110 to 170 $W \cdot m^{-2}K^{-1}$. Such performance is comparable or even better than the latent heat recovery from flue gas by a titanium heat exchanger [36].

3.2. Effect of water flow rate

Both water flux and heat flux increase with the increase in water flow rate (Fig. 3A). Similar findings in membrane condensation have been reported by Wang et al. [10]. This trend is most likely due to the significant boundary layer effect where laminar flow occurs due to the low water flow rate [33]. The water flow rate may have limited effect on water and heat fluxes when the water flow rate is sufficiently high (i.e. at turbulent flow when the boundary layer effect is insignificant) [23]. Since the tubular membrane in this study is relatively short (0.085 m), the temperature change between inlet and outlet water will not be detectable if the water flow rate is too high. Therefore, we maintained very low water flow rates in the experiment.

Water and heat recoveries improve slightly with the increase of the water flow rate (Fig. 3B). When the water flow rate increases from 1.1 to 9.8 $L \cdot h^{-1}$, water and heat recoveries increase from 35% to 47% and from 25% to 39%, respectively. It indicates that increasing the coolant flow rate can effectively improve the heat recovery efficiency, as confirmed by an analytical model [37]. The water and heat recoveries from unsaturated flue gas are also lower than those from saturated gas streams [19, 23].

The overall heat transfer coefficient goes up linearly with the increase in water flow rate (Fig. 3C). This suggests that increasing the coolant liquid flow rate can effectively improve the heat recovery performance of the membrane condenser. In large-scale plant operations, the water flow rate can be much higher than that in this lab-scale study. In other words, in industrial conditions, higher heat and water transfer rates and recoveries can be achieved due to the higher water flow rates. However, increasing water flow rates cannot result in unlimited but asymptotical increase in the transfer rate and recovery [32, 33, 38, 39]. Also, the rise in water flow rate increases the transmembrane pressure, which may influence the process performance.

3.3. Effect of inlet gas temperature

In the experiment, the humidity ratio and specific enthalpy of the flue gas are relatively stable (95 ± 5 $g \cdot kg^{-1}$ and 395 ± 5 $kJ \cdot kg^{-1}$, respectively) with the change in gas temperature. As the inlet gas temperature increases, water and heat fluxes across the membrane increase slightly (Fig. 4A). In the flue gas temperature range of 80 - 120 °C, water and heat fluxes are 4.8 - 6.5 $kg \cdot m^{-2}h^{-1}$ and 17 - 24 $MJ \cdot m^{-2}h^{-1}$, respectively. The water flux is slightly higher than that (~5.5 $kg \cdot m^{-2}h^{-1}$) in a similar study [10]. The flux improvement with increasing gas temperature results from the large temperature difference across the membrane as the driving force in the process.

Water and heat recoveries also improve with the rise in gas temperature (Fig. 4B). However, water recovery is much higher than heat recovery, particularly at higher gas temperatures. This phenomenon can be explained by the higher heat loss at higher gas temperatures in the bench-scale experiments. In a well thermally insulated plant operation, the heat recovery can be higher than that in this laboratory based study. In addition, increased water temperature at higher gas temperature can reduce the temperature difference across the membrane and thus lower the heat transfer efficiency. As a result, the overall heat transfer coefficient reduces with the rise in gas temperature (Fig. 4C). Thus, selecting water at low temperature as the liquid coolant can effectively improve the heat recovery.

3.4. Effect of inlet water temperature

Coolant water temperature plays an important role in both fluxes and recoveries (Figs. 5AB). The water flux declines from 5.5 to 3.6 $kg \cdot m^{-2}h^{-1}$ and the heat flux drops by approximately 10 times (from 20 to 2 $MJ \cdot m^{-2}h^{-1}$) when the inlet water temperature rises from 25 to 50 °C (Fig. 5A). Similarly, significant declines in water and heat recoveries are described in Fig. 5B. With increasing water temperature, the overall heat transfer coefficient also dramatically declines from 118 to 14 $W \cdot m^{-2}K^{-1}$ (Fig. 5C). It is obvious that heat transfer performance (heat flux, recovery and transfer coefficient) are very sensitive to the temperature change of the coolant (Fig. 5). Therefore, to maximize heat transfer performance, it is necessary to limit the coolant liquid temperature in the industrial operations.

3.5. Effect of flue gas humidity

Flue gas humidity also plays an important role in mass and heat transfer performance in the membrane condensation process (Figs. 6). When the gas humidity ratio increases from 17 to 120 $g \cdot kg^{-1}$, the corresponding water and heat fluxes increase from 0.7 to 8 $kg \cdot m^{-2}h^{-1}$, and from 9.2 to 25 $MJ \cdot m^{-2}h^{-1}$, respectively (Fig. 6A). The recovered water and heat fluxes are comparable with those using a hydrophobic porous membrane with a similar pore size (10 nm) but lower than those using a hydrophilic nanoporous membrane [17]. For example, when the relative humidity is ~ 16 vol.% (corresponding to a humidity ratio of 120 g/kg), our recovered water and heat fluxes are 8 $kg \cdot m^{-2}h^{-1}$ and 25 $MJ \cdot m^{-2}h^{-1}$, respectively; while they are 6 $kg \cdot m^{-2}h^{-1}$ and 23 $MJ \cdot m^{-2}h^{-1}$, respectively, using a hydrophobic porous membrane with a pore size of 10 nm in literature [17]. The slight difference in water and heat fluxes is mainly caused by the variation in the gas temperature and hydrophilicity of the membranes.

Water and heat recoveries show interesting changes. The water recovery ratio (~ 40%) in the present study is comparable with that in the industrial operation [10]. By elevating the flue gas humidity, the water recovery increases first and then levels off; while the heat recovery maintains relatively stable (Fig. 6B). This suggests that the flue gas humidity has minimal effect on water and heat recoveries.

Although the increase of flue gas humidity cannot obviously improve the water and heat recoveries, it can significantly increase the overall heat transfer coefficient due to the enhanced water and heat transfer rates (Fig. 6). In Fig. 6C, it can be seen that the overall heat transfer coefficient increases from 53 to 170 $W \cdot m^{-2}K^{-1}$ as the flue gas humidity raises from 16 to 120 $g \cdot kg^{-1}$. These results offer significant insights into optimizing the condensation performance in large-scale water and heat recovery operations.

3.6. How to optimise operational parameters?

The effect of operational parameters (fluid flow rates, temperatures and gas humidities) on the process performance is summarized in Table 1. Obviously, increasing gas flow rates will reduce the overall performance in water and heat recovery due to the decreased gas-membrane contact time. Particularly, water and heat recovery ratios drop significantly as the gas flow rate increases. However, increase of the coolant water flow rate can effectively improve the heat flux, water and heat recovery ratios and overall heat transfer coefficient due to the severe boundary layer effects at low water flow rates. In a practical operation, there should be an optimal water flow rate beyond which the overall performance in water and heat recovery cannot be improved obviously.

The rise in flue gas temperature can significantly enhance mass and heat transfer, leading to improved water and heat recovery ratios. Nevertheless, the overall heat transfer coefficient reduces as the flue gas temperature increases, which is most likely caused by the high heat loss at high temperatures. Increasing the coolant water temperature can significantly decrease the overall performance in water and heat recovery. Therefore, it is necessary to maintain a low coolant water temperature to maximize the water and heat recovery performance in practical operations. The water flux, heat flux and overall heat transfer coefficient increase obviously as the flue gas humidity rises. However, the water and heat recovery ratios are still relatively stable.

Overall, increasing the gas flow rate or water temperature has adverse impacts on the overall water and heat recovery performance. Increasing the water flow rate, flue gas temperature or humidity can favourably improve the overall performance in water and heat recovery.

4. Conclusion

This study demonstrates that the operational parameters, including fluid (gas and water) flow rates, temperatures of flue gas and coolant water, and flue gas humidity have significant effects on the process performance in terms of mass and heat transfer across the membrane condenser. As the gas flow rate increases, water and heat transfer efficiencies and recoveries decline due to the reduced residence time, suggesting that mass and heat transfers and recoveries can be enhanced when longer tubular membranes are employed. Increasing the water flow rate can effectively improve the mass and heat transfer efficiencies and recoveries.

Increasing the temperature of the inlet flue gas can enhance water and heat fluxes and recoveries, but does not improve the overall heat transfer efficiency. The coolant water temperature plays an important role in water and heat transfer efficiencies and recoveries. Lowering the coolant water temperature can dramatically improve the mass and heat transfer efficiencies and recoveries. Increasing the flue gas humidity can significantly improve water and heat transfer rates and the overall heat transfer coefficient, but has little effect on water and heat recoveries. The findings from this bench-scale investigation offer a general guideline in optimising the operational parameters in low-grade heat recovery with membrane heat exchangers. Economic analysis of this technology for flue gas water and heat recovery will be carried out in our future study.

Acknowledgements

The authors thank the financial support from the Open Research Fund Program of Collaborative Innovation Center of Membrane Separation and Water Treatment (2016YB01), the National Natural Science Foundation of China (21276123, 51676080), and the "Summit of the Six Top Talents" Program of Jiangsu Province. Special thanks also go to Drs Dexin Wang, Lixin Xue and Simin Huang, and Professor Damian Gore for the helpful discussion and revision during manuscript preparation.

References

[1] F.N. Al-Mousawi, R. Al-Dadah, S. Mahmoud, Low grade heat driven adsorption system for cooling and power generation using advanced adsorbent materials, Energy Conversion and Management, 126 (2016) 373-384.

[2] S. Maalouf, E. Boulawz Ksayer, D. Clodic, Investigation of direct contact condensation for wet flue-gas waste heat recovery using Organic Rankine Cycle, Energy Conversion and Management, 107 (2016) 96-102.

[3] M. Terhan, K. Comakli, Design and economic analysis of a flue gas condenser to recover latent heat from exhaust flue gas, Applied Thermal Engineering, 100 (2016) 1007-1015.

[4] X. Han, J. Yan, S. Karellas, M. Liu, E. Kakaras, F. Xiao, Water extraction from high moisture lignite by means of efficient integration of waste heat and water recovery technologies with flue gas pre-drying system, Applied Thermal Engineering, 110 (2017) 442-456.

[5] G. Xu, S. Huang, Y. Yang, Y. Wu, K. Zhang, C. Xu, Techno-economic analysis and optimization of the heat recovery of utility boiler flue gas, Applied Energy, 112 (2013) 907-917.

[6] S. Judd, B. Jefferson, Membranes for industrial wastewater recovery and re-use, Elsevier, 2003.

[7] Water Capture, in, http://www.watercapture.eu/.

[8] D. Wang, Transport membrane condenser for water and energy recovery from power plant flue gas, Final technical report, Gas Technology Institute, 2012.

[9] BCS, Incorparated, Waste heat recovery: technology and opportunities in US industry, U.S. Department of Energy, 2008.

[10] D. Wang, A. Bao, W. Kunc, W. Liss, Coal power plant flue gas waste heat and water recovery, Applied Energy, 91 (2012) 341-348.

[11] B.F. Tchanche, G. Lambrinos, A. Frangoudakis, G. Papadakis, Low-grade heat conversion into power using organic Rankine cycles - A review of various applications, Renewable and Sustainable Energy Reviews, 15 (2011) 3963-3979.

[12] J. Zhang, Y. Zhou, Y. Li, G. Hou, F. Fang, Generalized predictive control applied in waste heat recovery power plants, Applied Energy, 102 (2013) 320-326.

[13] L. Westerlund, R. Hermansson, J. Fagerström, Flue gas purification and heat recovery: A biomass fired boiler supplied with an open absorption system, Applied Energy, 96 (2012) 444-450.

[14] Y. Li, M. Yan, L. Zhang, G. Chen, L. Cui, Z. Song, J. Chang, C. Ma, Method of flash evaporation and condensation - heat pump for deep cooling of coal-fired power plant flue gas: Latent heat and water recovery, Applied Energy, 172 (2016) 107-117.

[15] A. Messerer, V. Schmatloch, U. Pöschl, R. Niessner, Combined particle emission reduction and heat recovery from combustion exhaust - A novel approach for small wood-fired appliances, Biomass and Bioenergy, 31 (2007) 512-521.

[16] A. Gröhn, V. Suonmaa, A. Auvinen, K.E.J. Lehtinen, J. Jokiniemi, Reduction of Fine Particle Emissions from Wood Combustion with Optimized Condensing Heat Exchangers, Environmental Science & Technology, 43 (2009) 6269-6274.

[17] H.W. Hu, G.H. Tang, D. Niu, Wettability modified nanoporous ceramic membrane for simultaneous residual heat and condensate recovery, Scientific Reports, 6 (2016) 27274.

[18] A. Bao, D. Wang, C.-X. Lin, Nanoporous membrane tube condensing heat transfer enhancement study, International Journal of Heat and Mass Transfer, 84 (2015) 456-462.

[19] M. Yue, S. Zhao, P.H.M. Feron, H. Qi, Multichannel Tubular Ceramic Membrane for Water and Heat Recovery from Waste Gas Streams, Industrial & Engineering Chemistry Research, 55 (2016) 2615-2622.

[20] F. Macedonio, A. Brunetti, G. Barbieri, E. Drioli, Membrane Condenser as a New Technology for Water Recovery from Humidified "Waste" Gaseous Streams, Industrial & Engineering Chemistry Research, 52 (2012) 1160-1167.

[21] A. Brunetti, S. Santoro, F. Macedonio, A. Figoli, E. Drioli, G. Barbieri, Waste Gaseous Streams: From Environmental Issue to Source of Water by Using Membrane Condensers, CLEAN - Soil, Air, Water, 42 (2014) 1145-1153.

[22] E. Drioli, S. Santoro, S. Simone, G. Barbieri, A. Brunetti, F. Macedonio, A. Figoli, ECTFE membrane preparation for recovery of humidified gas streams using membrane condenser, Reactive and Functional Polymers, 79 (2014) 1-7.

[23] H. Chen, Y. Zhou, S. Cao, X. Li, X. Su, L. An, D. Gao, Heat exchange and water recovery experiments of flue gas with using nanoporous ceramic membranes, Applied Thermal Engineering, 110 (2017) 686-694.

[24] M.M. DeBusk, B. Bischoff, J. Hunter, J. Klett, E. Nafziger, S. Daw, Understanding the Effect of Dynamic Feed Conditions on Water Recovery from IC Engine Exhaust by Capillary Condensation with Inorganic Membranes, F. Dogan, T.M. Tritt, T. Sekino, Y. Katoh, A.J. Pyzik, l. Belharouak, A.R. Boccaccini, J. Marra, H.-T. Lin (eds.) Ceramics for Environmental and Energy Applications II, John Wiley & Sons, Inc., 2014, pp. 141-152.

[25] S. Yan, S. Zhao, L.T. Wardhaugh, P.H.M. Feron, Innovative use of membrane contactor as condenser for heat recovery in carbon capture, Environmental Science & Technology, (2015).

[26] F. Macedonio, M. Cersosimo, A. Brunetti, G. Barbieri, E. Drioli, Water recovery from humidified waste gas streams: Quality control using membrane condenser technology, Chemical Engineering and Processing: Process Intensification, 86 (2014) 196-203.

[27] T. Wang, M. Yue, H. Qi, P.H.M. Feron, S. Zhao, Transport membrane condenser for water and heat recovery from gaseous streams: Performance evaluation, Journal of Membrane Science, 484 (2015) 10-17.

[28] J. Sekulic-Kuzmanovic, Mesoporous and microporous titania membranes, PhD thesis, University of Twente, Enschede, 2004.

[29] H. Qi, S. Niu, X. Jiang, N. Xu, Enhanced performance of a macroporous ceramic support for nanofiltration by using α-Al_2O_3 with narrow size distribution, Ceramics International, 39 (2013) 2463-2471.

[30] E. Jakobs, W.J. Koros, Ceramic membrane characterization via the bubble point technique, Journal of Membrane Science, 124 (1997) 149-159.

[31] J. Feng, Y. Fan, H. Qi, N. Xu, Co-sintering synthesis of tubular bilayer α-alumina membrane, Journal of Membrane Science, 288 (2007) 20-27.

[32] S. Zhao, P.H.M. Feron, Z. Xie, J. Zhang, M. Hoang, Condensation studies in membrane evaporation and sweeping gas membrane distillation, Journal of Membrane Science, 462 (2014) 9-16.

[33] S. Zhao, C. Cao, L. Wardhaugh, P.H.M. Feron, Membrane evaporation of amine solution for energy saving in post-combustion carbon capture: Performance evaluation, Journal of Membrane Science, 473 (2015) 274-282.

[34] M. Khayet, M.P. Godino, J.I. Mengual, Thermal boundary layers in sweeping gas membrane distillation processes, AIChE Journal, 48 (2002) 1488-1497.

[35] M. Khayet, P. Godino, J.I. Mengual, Theory and experiments on sweeping gas membrane distillation, Journal of Membrane Science, 165 (2000) 261-272.

[36] K. Hwang, C.h. Song, K. Saito, S. Kawai, Experimental study on titanium heat exchanger used in a gas fired water heater for latent heat recovery, Applied Thermal Engineering, 30 (2010) 2730-2737.

[37] K. Jeong, M.J. Kessen, H. Bilirgen, E.K. Levy, Analytical modeling of water condensation in condensing heat exchanger, International Journal of Heat and Mass Transfer, 53 (2010) 2361-2368.

[38] Z. Xie, T. Duong, M. Hoang, C. Nguyen, B. Bolto, Ammonia removal by sweep gas membrane distillation, Water Research, 43 (2009) 1693-1699.

[39] S. Zhao, L. Wardhaugh, J. Zhang, P.H.M. Feron, Condensation, re-evaporation and associated heat transfer in membrane evaporation and sweeping gas membrane distillation, Journal of Membrane Science, 475 (2015) 445-454.

Figure captions

Fig. 1. Schematic diagram of the experimental setup for artificial flue gas generation and heat and water recovery. H = Humidity transmitter, T = thermocouple. Data from the humidity transmitter, thermocouple and balance are recorded with relevant softwares on a computer.

Fig. 2. Effect of gas flow rate on (A) water and heat fluxes, (B) gas humidity ratio and specific enthalpy, (C) water and heat recoveries, and (D) overall heat transfer coefficient. Experimental conditions: inlet gas stream temperature 100 °C; liquid water flow rate 3.3 $L \cdot h^{-1}$; liquid side gauge pressure 0 bar; gas side gauge pressure 0.1 bar; effective membrane area 0.0021 m^2.

Fig. 3. Effect of water flow rate on (A) water and heat fluxes, (B) water and heat recoveries, and (C) overall heat transfer coefficient. Experimental conditions: inlet gas stream temperature 100 °C; gas flow rate 4.1 $L \cdot min^{-1}$; liquid side gauge pressure 0 bar; gas side gauge pressure 0.1 bar; effective membrane area 0.0021 m^2.

Fig. 4. Effect of inlet gas temperature on water and heat (A) fluxes, (B) recoveries, and (C) overall heat transfer coefficient. Experimental conditions: inlet gas flow rate 5.4 $L \cdot min^{-1}$; liquid water flow rate 3.3 $L \cdot h^{-1}$; liquid side gauge pressure 0 bar; gas side gauge pressure 0.1 bar; effective membrane area 0.0021 m^2.

Fig. 5. Effect of inlet liquid temperature on water and heat (A) fluxes, (B) recoveries, and (C) overall heat transfer coefficient. Experimental conditions: inlet gas stream temperature 100 °C; gas flow rate 5.4 $L \cdot min^{-1}$; liquid water flow rate 3.3 $L \cdot h^{-1}$; liquid side gauge pressure 0 bar; gas side gauge pressure 0.2 bar; effective membrane area 0.0021 m^2.

Fig. 6. Effect of inlet gas humidity on water and heat (A) fluxes, (B) recoveries, and (C) overall heat transfer coefficient. Experimental conditions: inlet gas stream temperature 100 °C; gas flow rate 5.4 $L \cdot min^{-1}$; liquid water flow rate 3.3 $L \cdot h^{-1}$; liquid side gauge pressure 0 bar; gas side gauge pressure 0.1 bar; effective membrane area 0.0021 m^2.

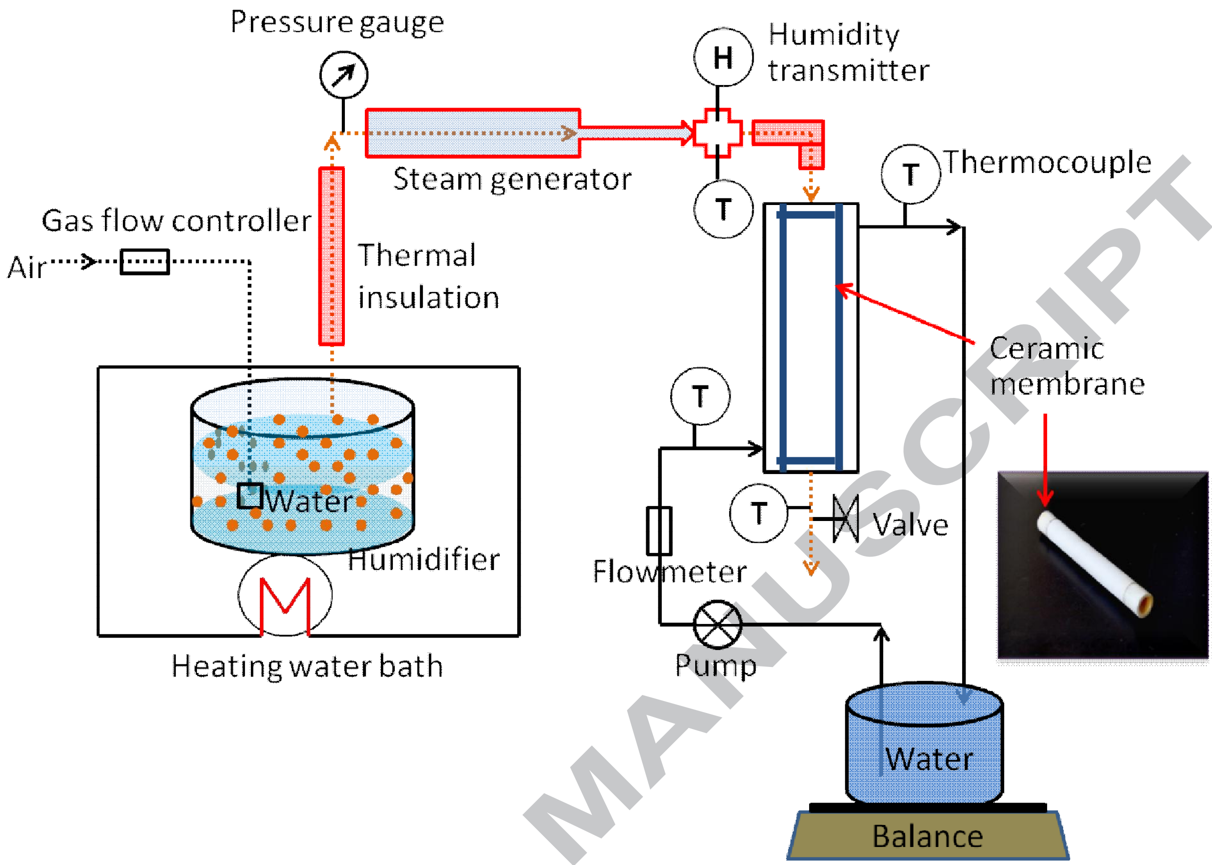

Fig. 1. Schematic diagram of the experimental setup for artificial flue gas generation and heat and water recovery. H = Humidity transmitter, T = thermocouple. Data from the humidity transmitter, thermocouple and balance are recorded with relevant softwares on a computer.

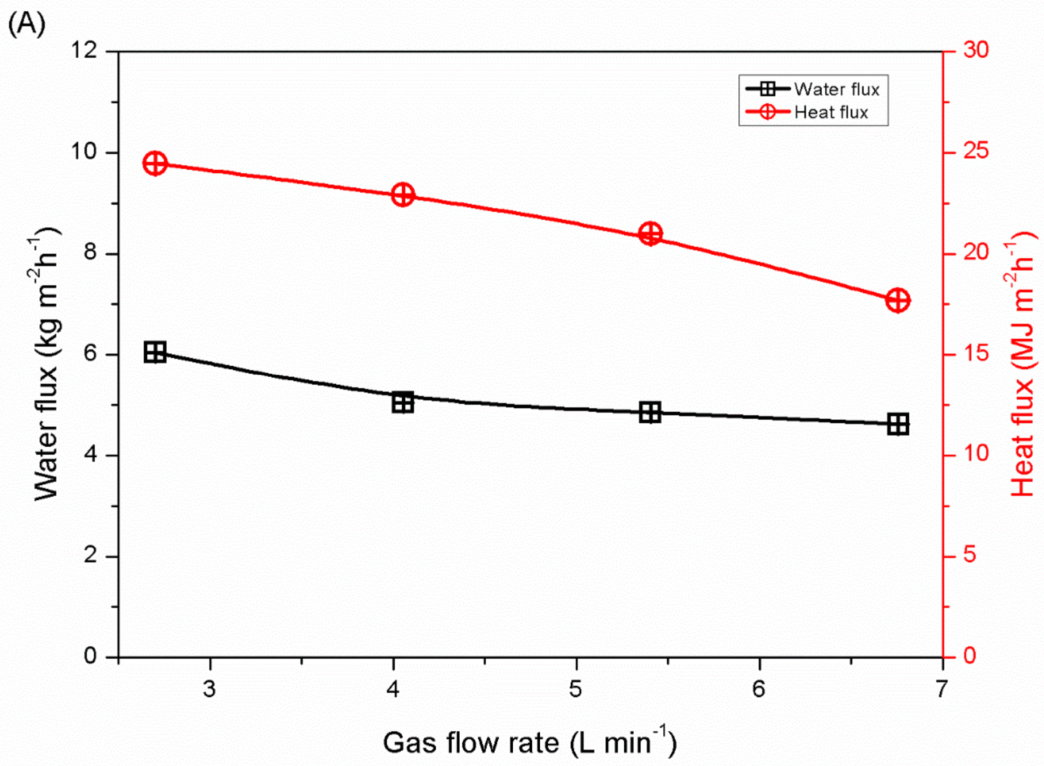
(A)
Water flux
Heat flux
Water flux (kg m-2h-1)
Heat flux (MJ m-2h-1)
Gas flow rate (L min-1)

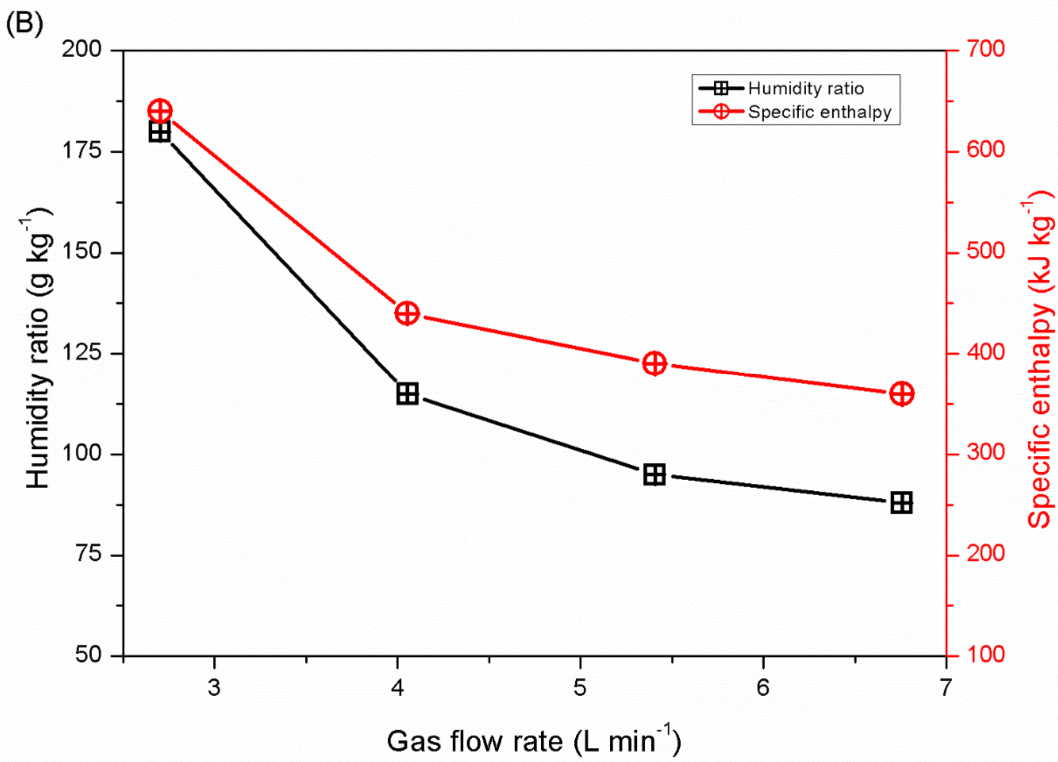
(B)
Humidity ratio
Specific enthalpy
Humidity ratio (g kg-1)
Specific enthalpy (kJ kg-1)
Gas flow rate (L min-1)

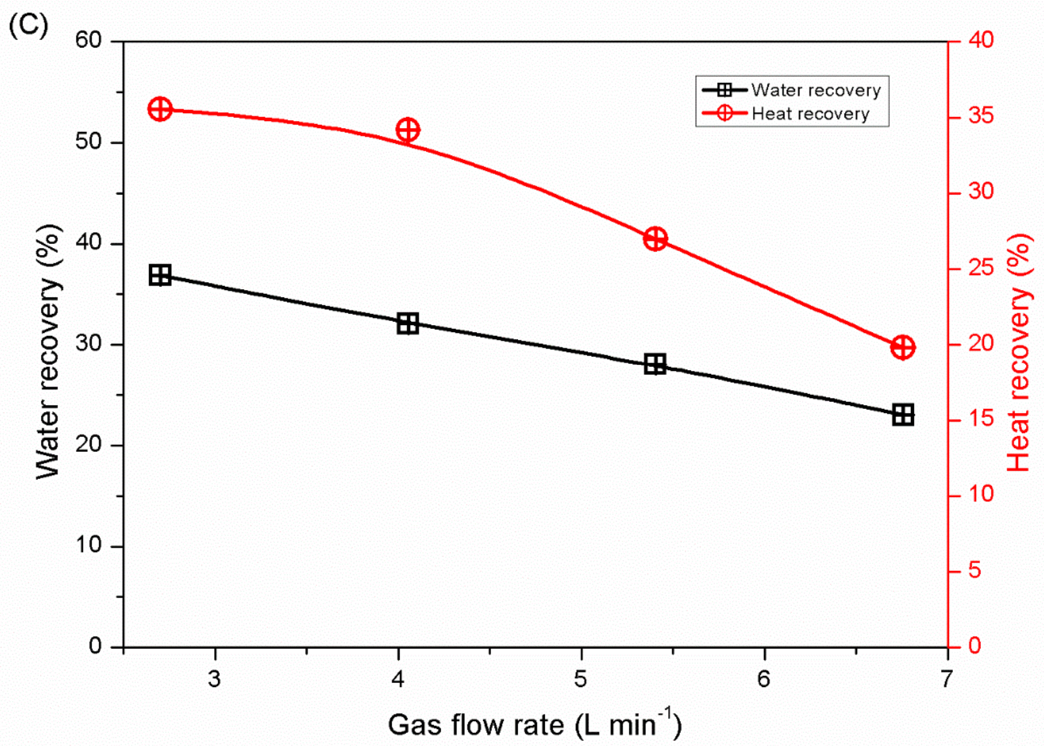
(C)
Water recovery
Heat recovery
Water recovery (%)
Heat recovery (%)
Gas flow rate (L min^{-1})
0
10
20
30
40
50
60
0
5
10
15
20
25
30
35
40
3
4
5
6
7

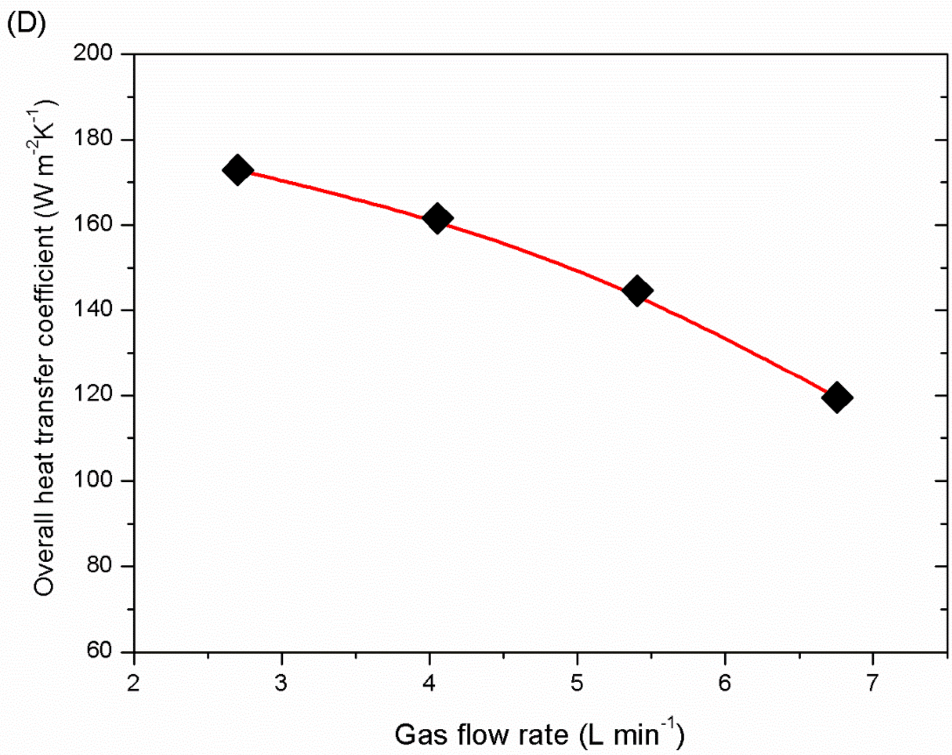
(D)
Overall heat transfer coefficient (W m^{-2}K^{-1})
Gas flow rate (L min^{-1})
60
80
100
120
140
160
180
200
2
3
4
5
6
7

Fig. 2. Effect of gas flow rate on (A) water and heat fluxes, (B) gas humidity ratio and specific enthalpy, (C) water and heat recoveries, and (D) overall heat transfer coefficient. Experimental conditions: inlet gas stream temperature 100 °C; liquid water flow rate 3.3 $L\cdot h^{-1}$; liquid side gauge pressure 0 bar; gas side gauge pressure 0.1 bar; effective membrane area 0.0021 m^2.

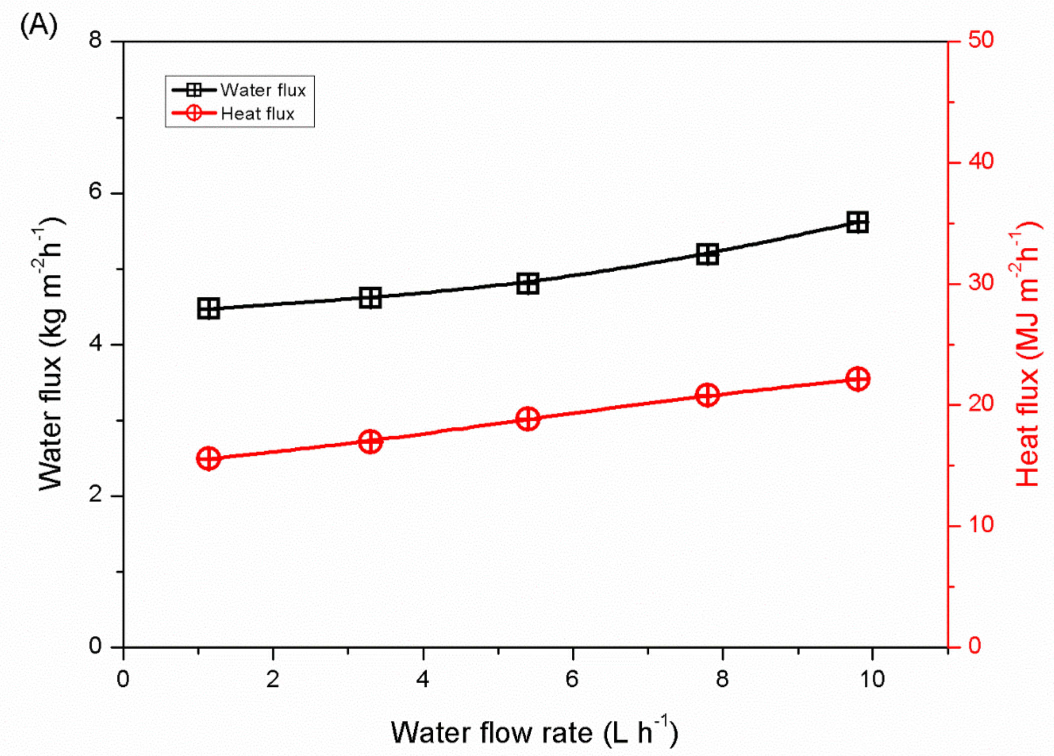
(A)
Water flux
Heat flux
Water flux (kg m-2h-1)
Heat flux (MJ m-2h-1)
Water flow rate (L h-1)
0
2
4
6
8
10
10
20
30
40
50

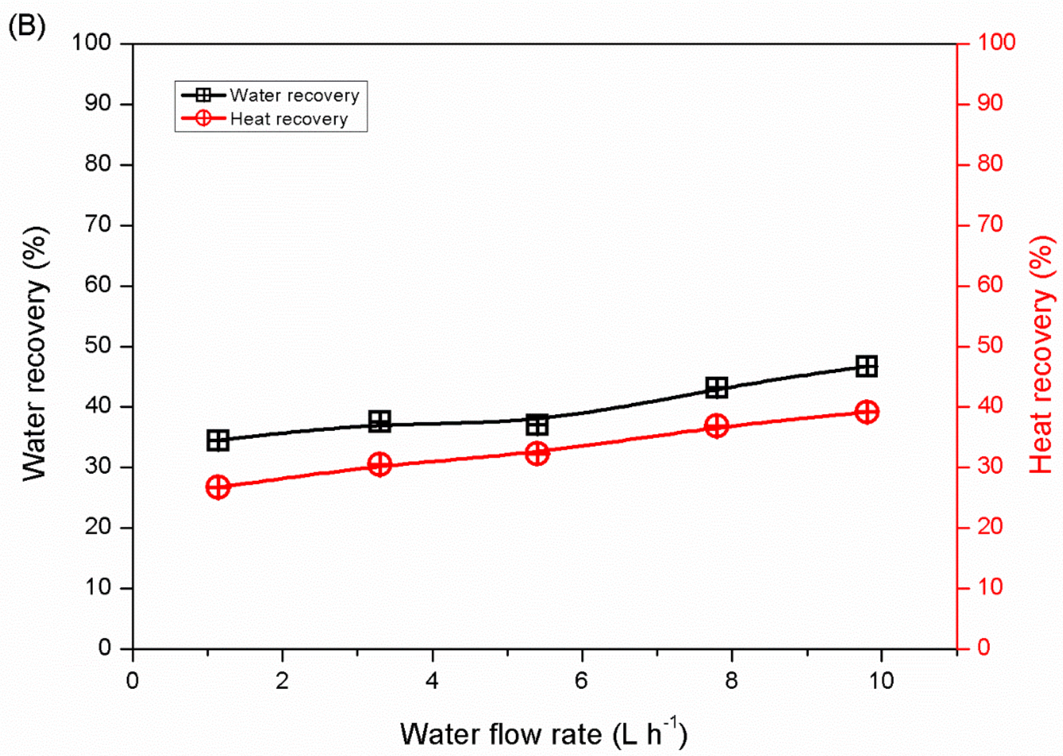
(B)
Water recovery
Heat recovery
Water recovery (%)
Heat recovery (%)
Water flow rate (L h-1)
0
10
20
30
40
50
60
70
80
90
100
2
4
6
8

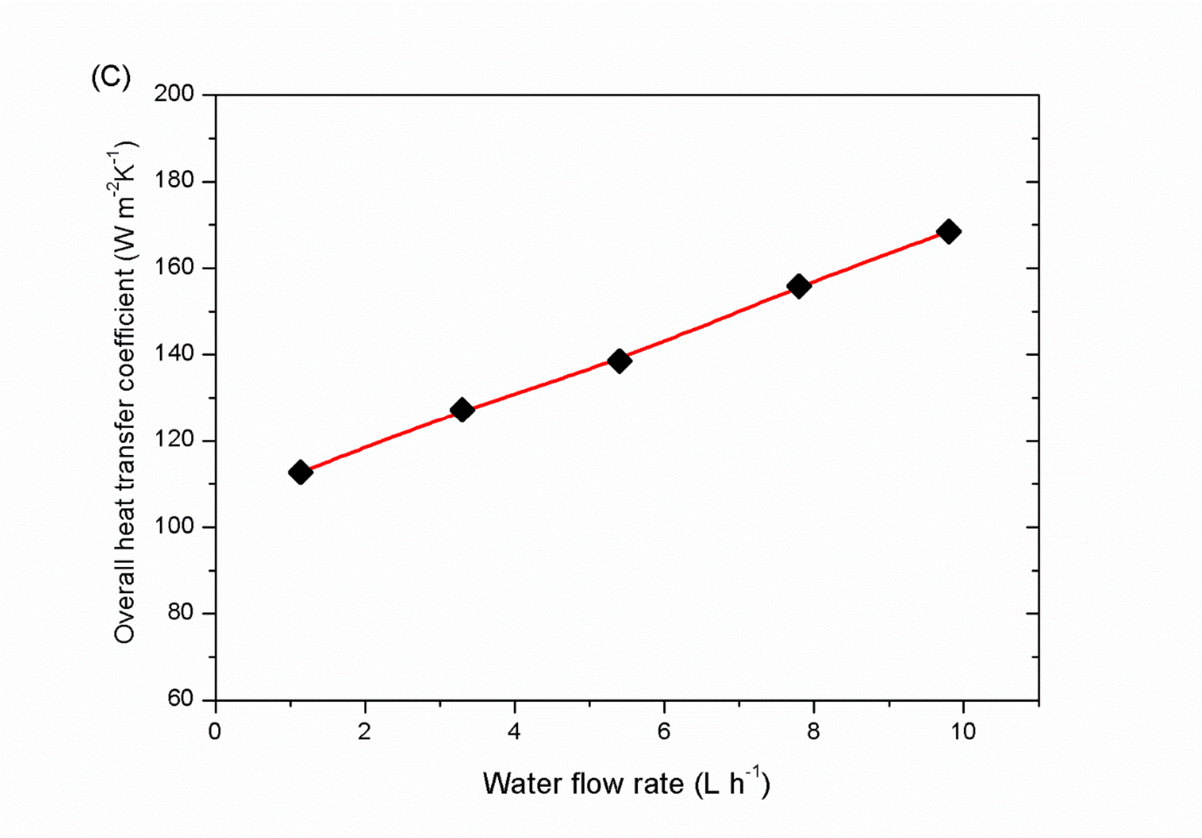

Fig. 3. Effect of water flow rate on (A) water and heat fluxes, (B) water and heat recoveries, and (C) overall heat transfer coefficient. Experimental conditions: inlet gas stream temperature 100 °C; gas flow rate 4.1 $L \cdot min^{-1}$; liquid side gauge pressure 0 bar; gas side gauge pressure 0.1 bar; effective membrane area 0.0021 m^2.

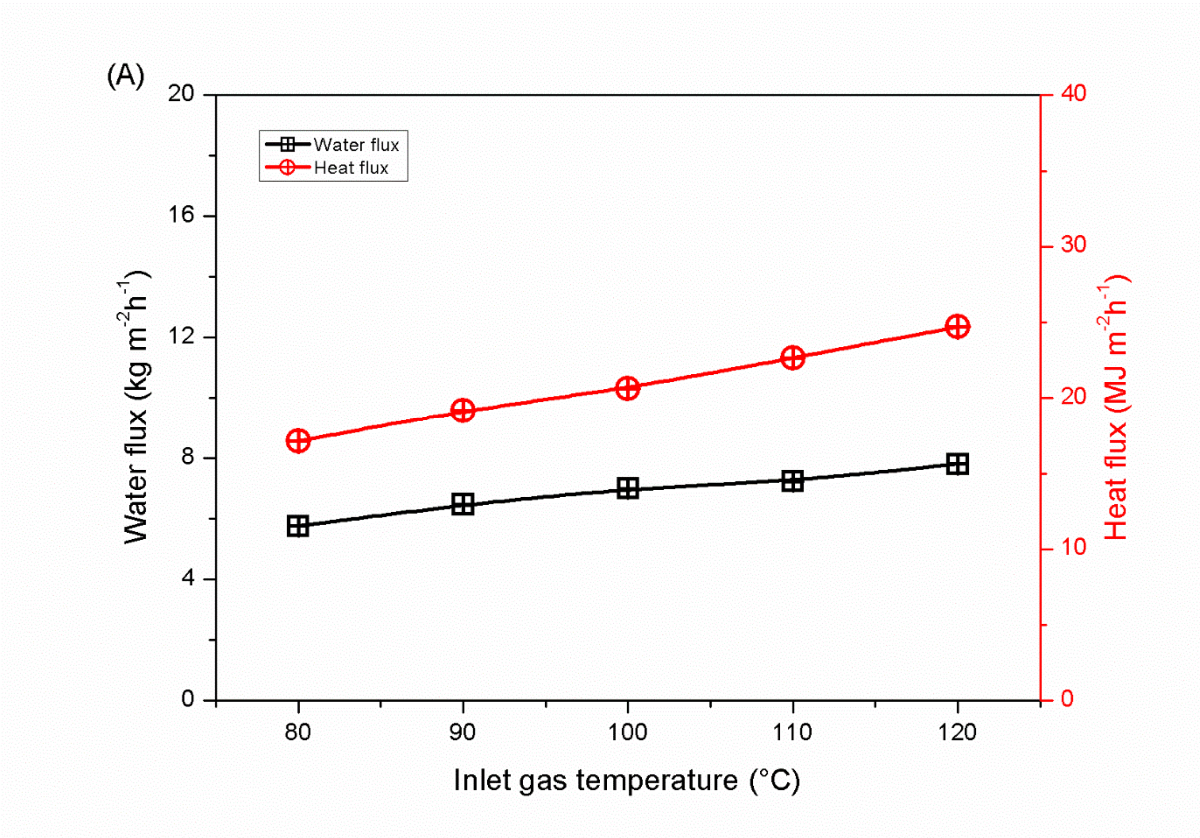
(A)
Water flux
Heat flux
Water flux (kg m-2h-1)
Heat flux (MJ m-2h-1)
Inlet gas temperature (°C)
0
4
8
12
16
20
0
10
20
30
40
80
90
100
110
120

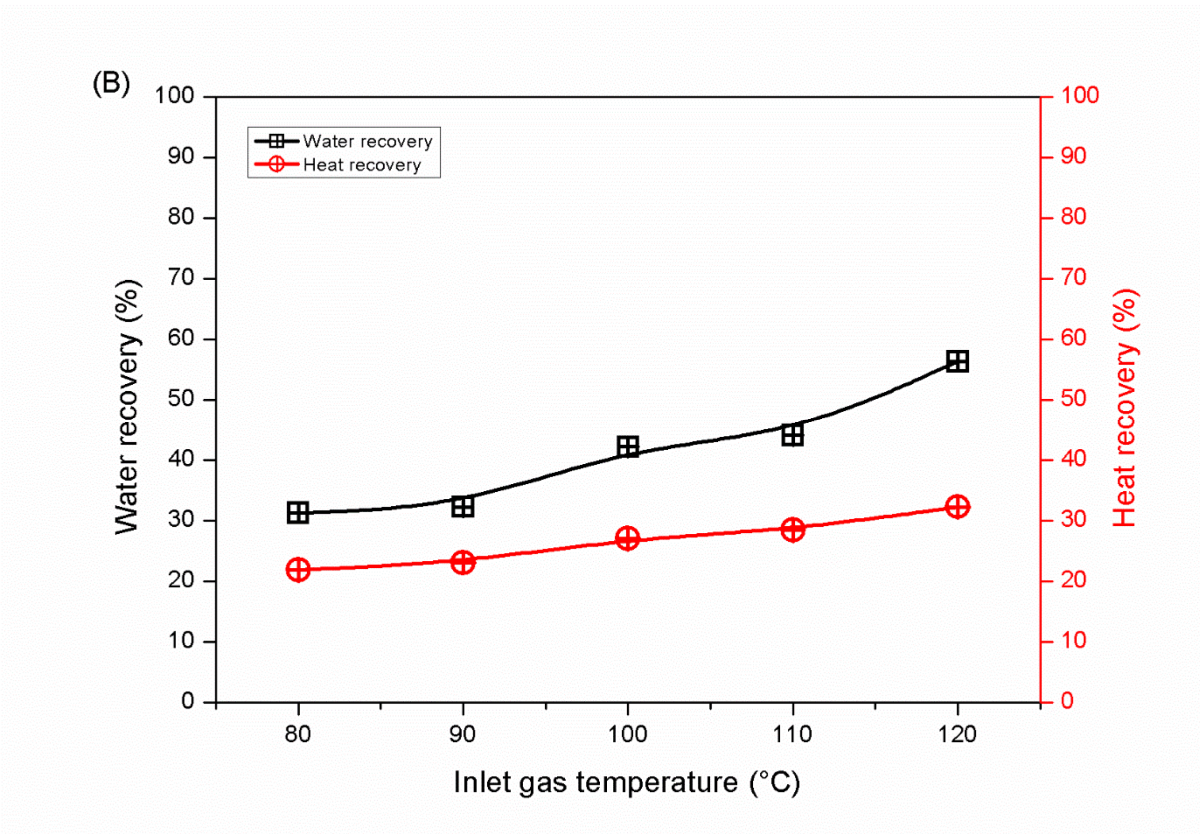
(B)
Water recovery
Heat recovery
Water recovery (%)
Heat recovery (%)
Inlet gas temperature (°C)
0
10
20
30
40
50
60
70
80
90
100
80
90
100
110
120

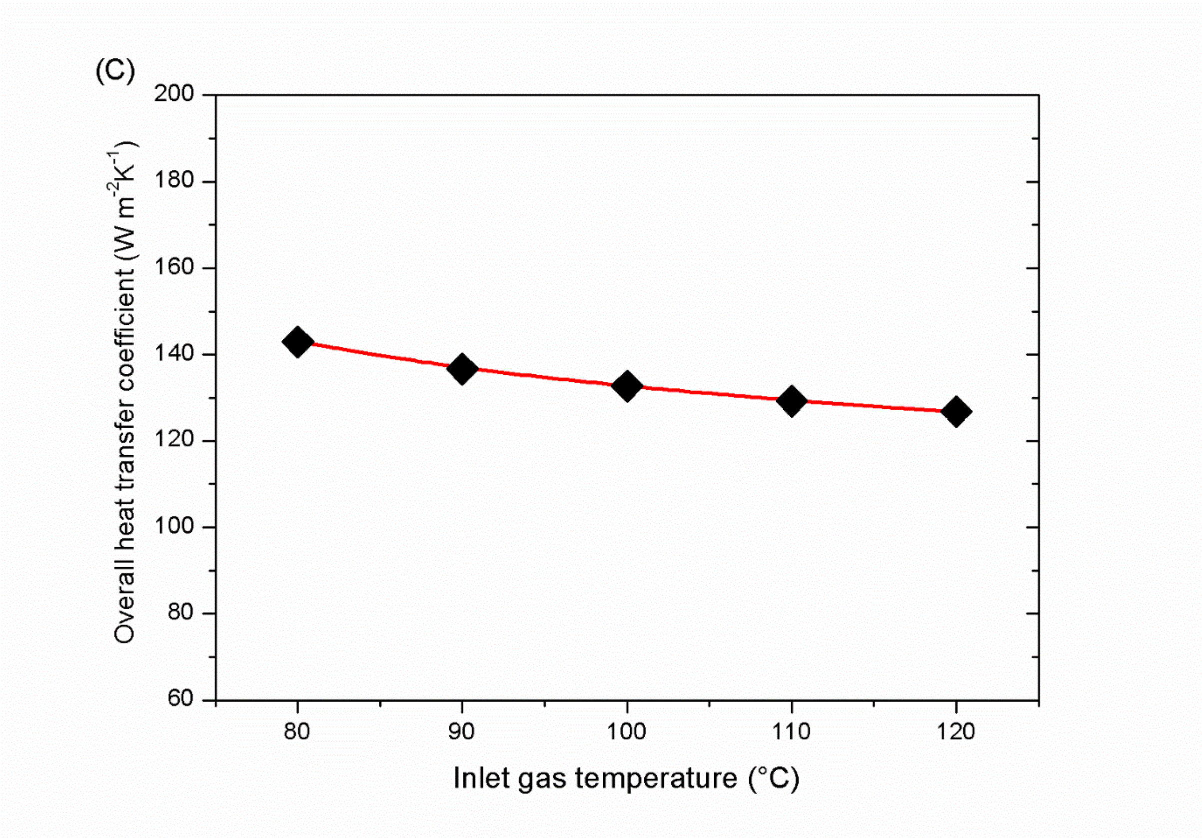

Fig. 4. Effect of inlet gas temperature on water and heat (A) fluxes, (B) recoveries, and (C) overall heat transfer coefficient. Experimental conditions: inlet gas flow rate 5.4 $L \cdot min^{-1}$; liquid water flow rate 3.3 $L \cdot h^{-1}$; liquid side gauge pressure 0 bar; gas side gauge pressure 0.1 bar; effective membrane area 0.0021 m^2.

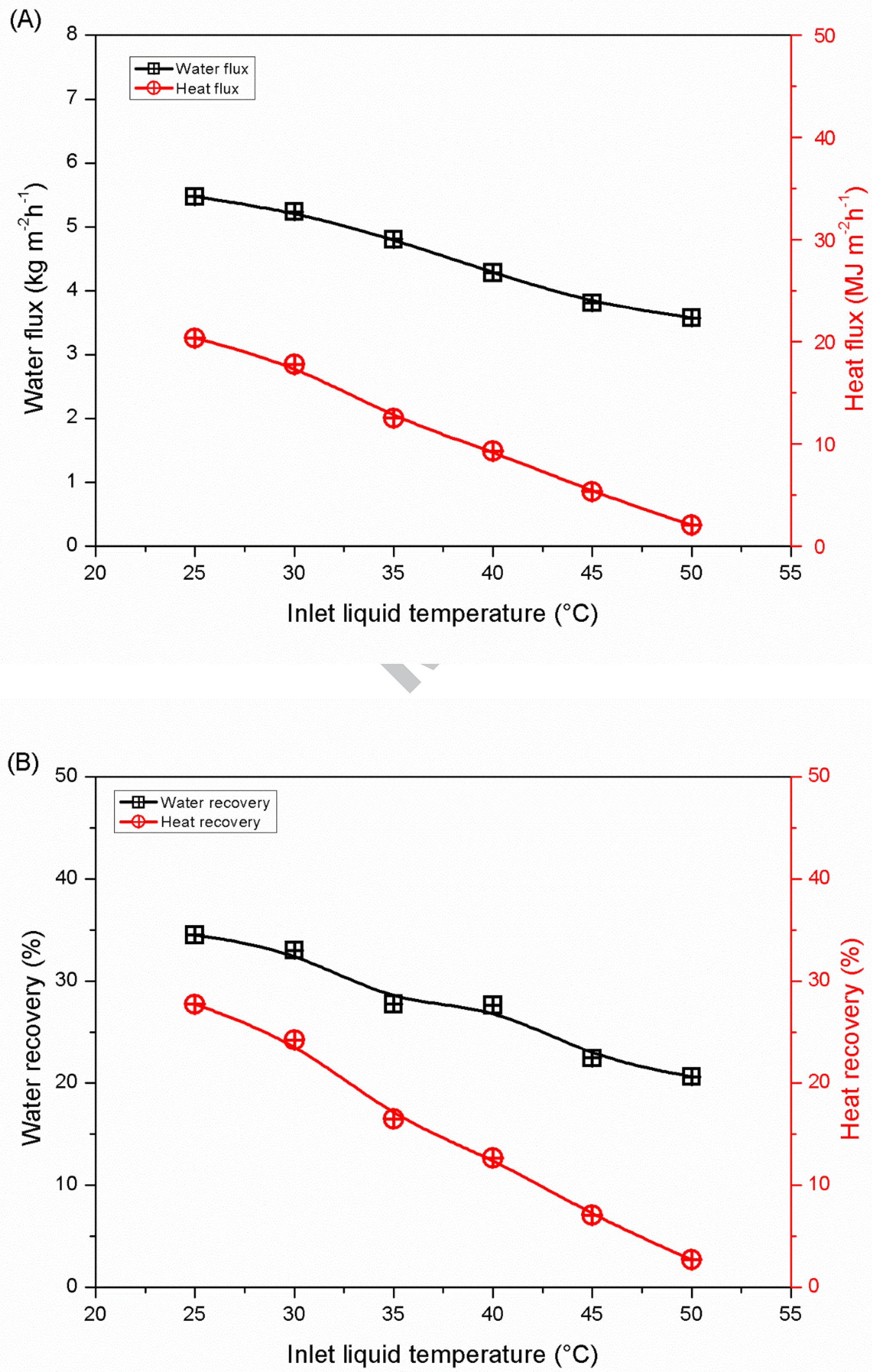
(A)
Water flux
Heat flux
Water flux (kg m-2h-1)
Heat flux (MJ m-2h-1)
Inlet liquid temperature (°C)
(B)
Water recovery
Heat recovery
Water recovery (%)
Heat recovery (%)
Inlet liquid temperature (°C)

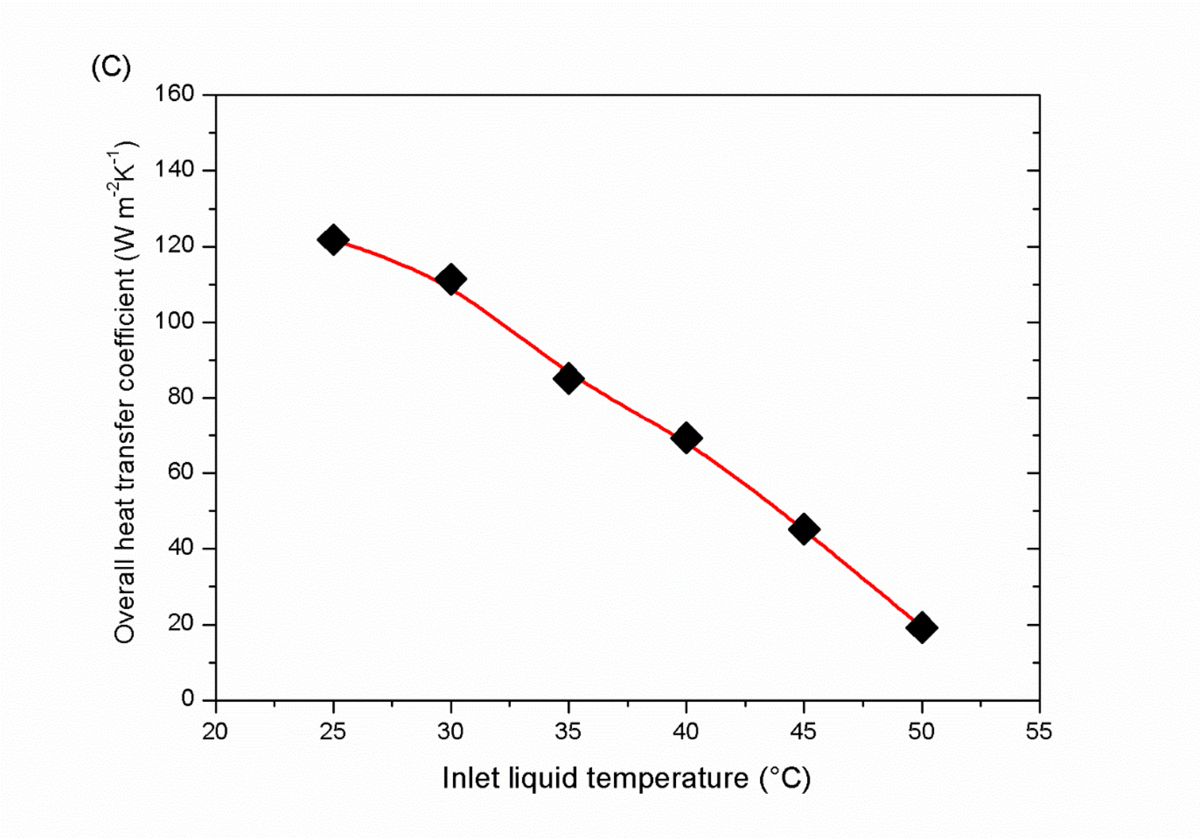

Fig. 5. Effect of inlet liquid temperature on water and heat (A) fluxes, (B) recoveries, and (C) overall heat transfer coefficient. Experimental conditions: inlet gas stream temperature 100 °C; gas flow rate 5.4 $L \cdot min^{-1}$; liquid water flow rate 3.3 $L \cdot h^{-1}$; liquid side gauge pressure 0 bar; gas side gauge pressure 0.2 bar; effective membrane area 0.0021 m^2.

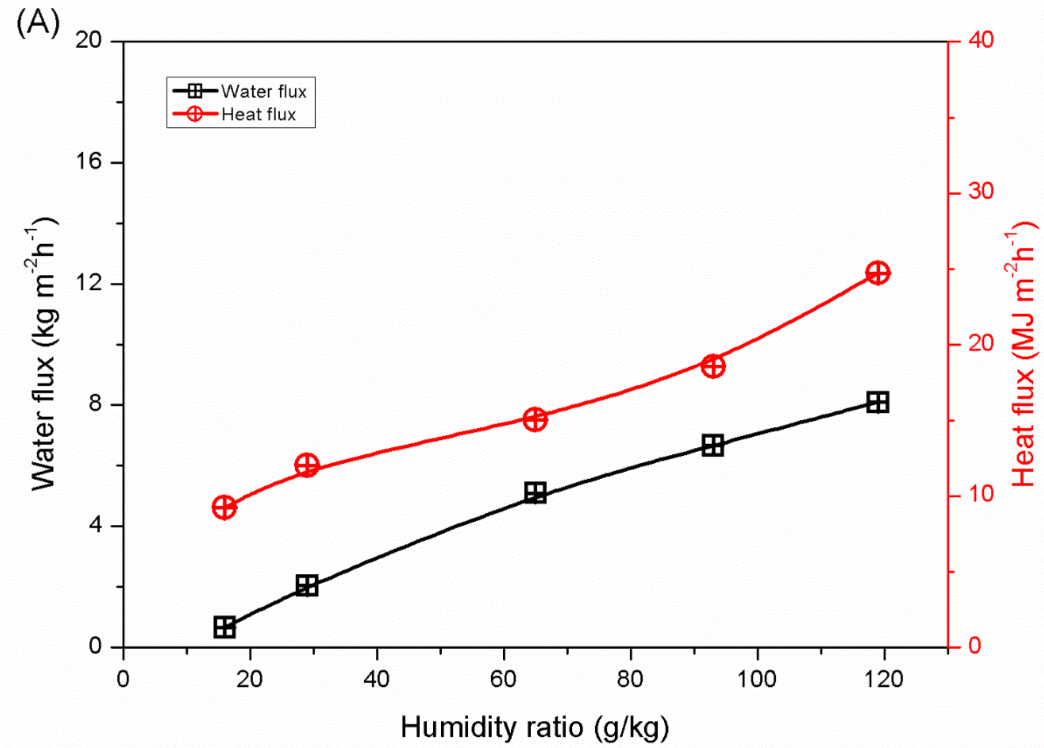
(A)
Water flux
Heat flux
Water flux (kg m^-2h^-1)
Heat flux (MJ m^-2h^-1)
Humidity ratio (g/kg)
0
4
8
12
16
20
0
10
20
30
40
0
20
40
60
80
100
120

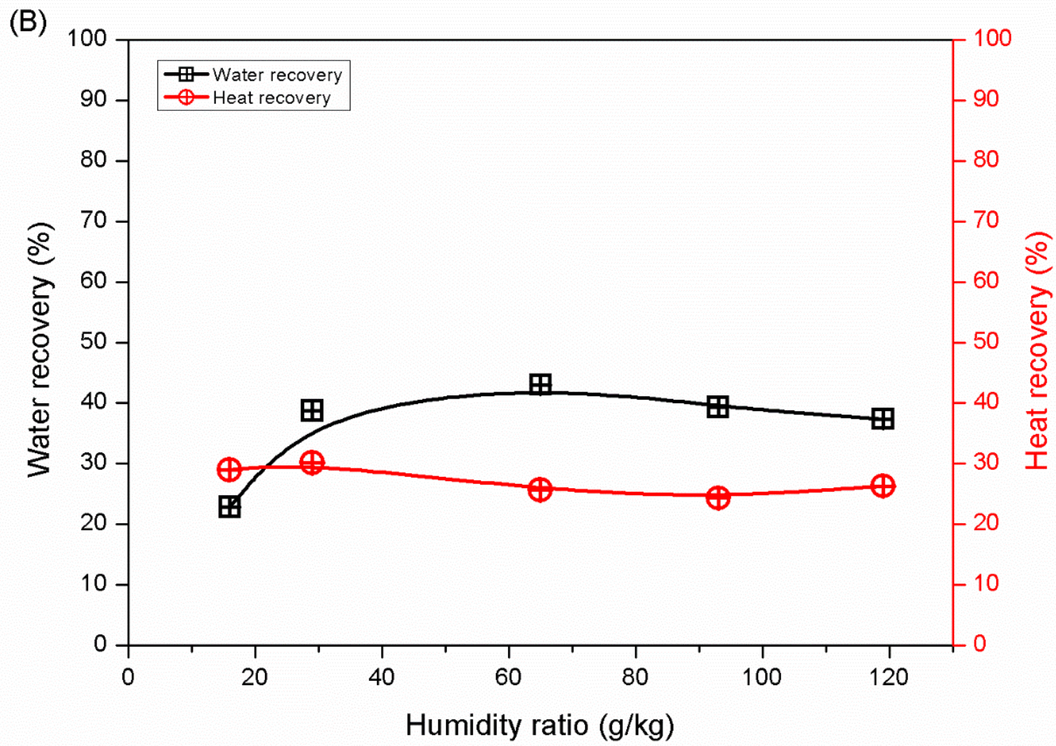
(B)
Water recovery
Heat recovery
Water recovery (%)
Heat recovery (%)
Humidity ratio (g/kg)
0
10
20
30
40
50
60
70
80
90
100
0
20
40
60
80
100
120

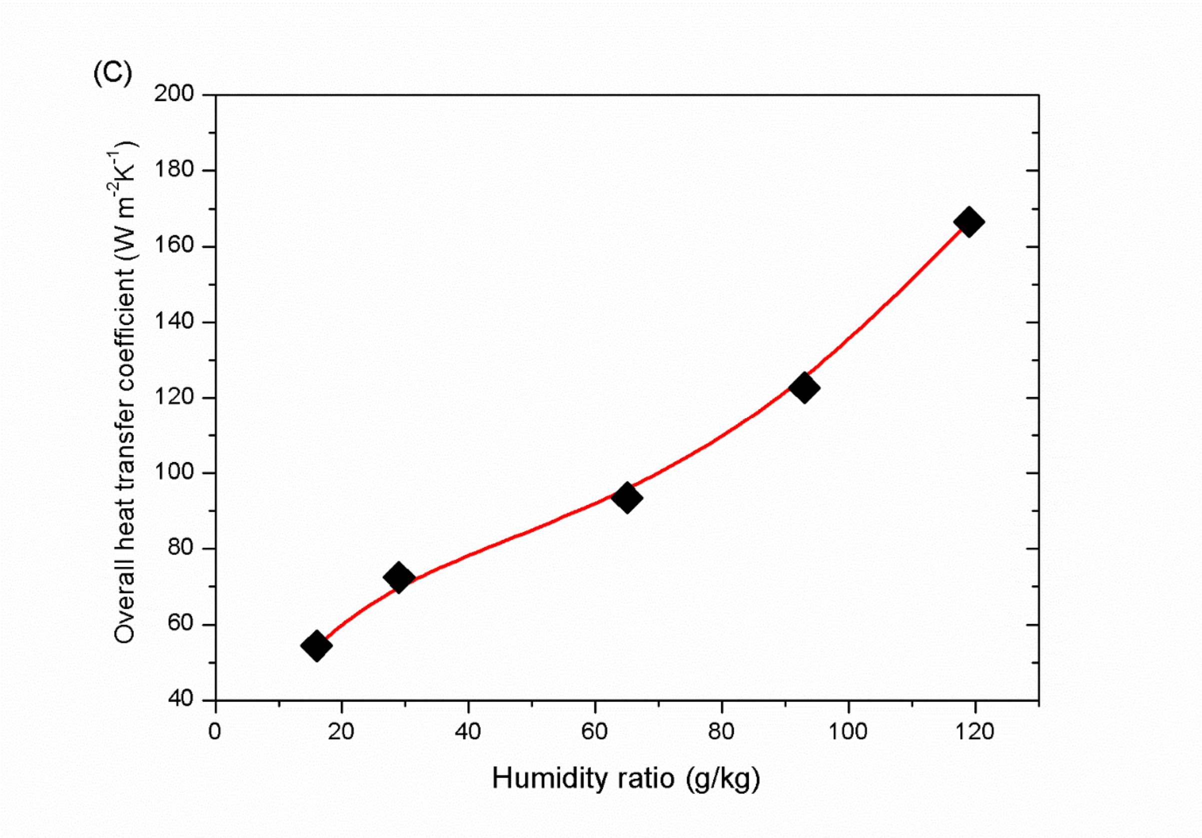

Fig. 6. Effect of inlet gas humidity on water and heat (A) fluxes, (B) recoveries, and (C) overall heat transfer coefficient. Experimental conditions: inlet gas stream temperature 100 °C; gas flow rate 5.4 L·min^{-1}; liquid water flow rate 3.3 L·h^{-1}; liquid side gauge pressure 0 bar; gas side gauge pressure 0.1 bar; effective membrane area 0.0021 m^2.

Table 1. Summary of the effect of operational parameters on process performance in membrane condensation.

Performance parameters	Operational parameters				
	Gas flow rates: 2.7 - 6.8 $L \cdot min^{-1}$	Water flow rates: 1.0 -10 $L \cdot h^{-1}$	Inlet gas temperatures: 80 - 120 °C	Inlet water temperatures: 25 - 50 °C	Humidity ratios: 16 - 120 $g \cdot kg^{-1}$
Water flux	-	+	++	--	++
Heat flux	-	++	++	--	++
Water recovery	--	++	++	--	RS
Heat recovery	--	++	++	--	RS
Overall heat transfer coefficient	--	++	-	--	++

++: increased by more than 30%.

+: increased by less than 30% but more than 10%.

--: decreased by more than 30%.

-: decreased by less than 30% but more than 10%

RS: relatively stable (increased or decreased by less than 10%).

Highlights:

1. Membrane condenser for water and heat recovery from flue gas is investigated;

2. Effect of operational parameters on overall heat transfer coefficient is studied;

3. Rise in gas flow rate or water temperature reduces overall recovery performance;

4. Rise in water flow rate, gas temperature or humidity improves overall performance;

5. This study offers a guideline in optimising parameters in membrane condensers.

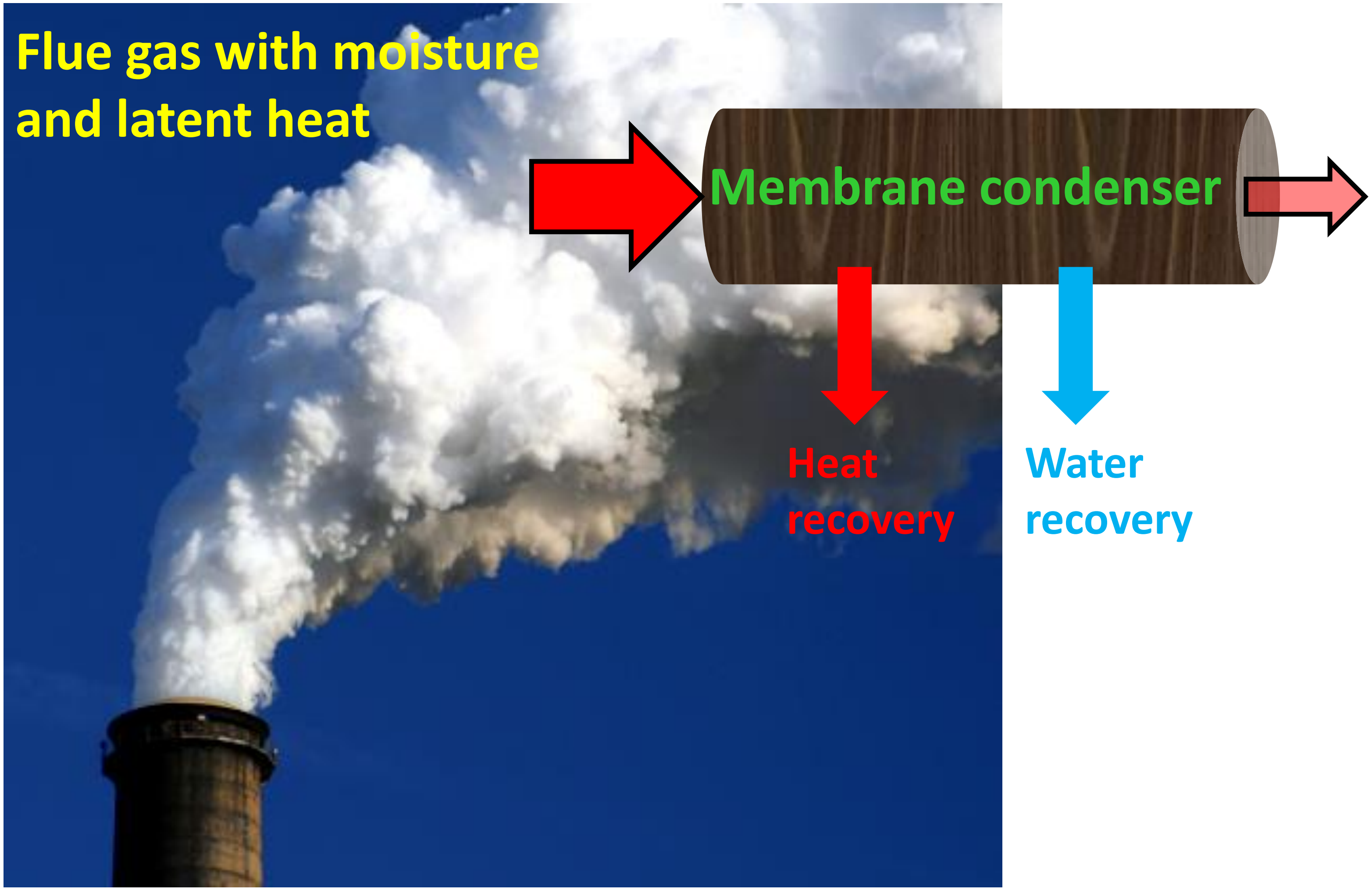
Flue gas with moisture and latent heat
Membrane condenser
Heat recovery
Water recovery